



Variations of the Somali upwelling since 18.5 ka BP and its relationship with southwest monsoon rainfall

Durairaj Balaji^{1,2}, Ravi Bhushan², and Laxman Singh Chamyal¹

¹Department of Geology, The Maharaja Sayajirao University of Baroda, India

²Geoscience Division, Physical Research Laboratory, Ahmedabad, India

Correspondence: Durairaj Balaji (balaji.d86@gmail.com)

Received: 6 June 2017 – Discussion started: 7 July 2017

Revised: 2 August 2018 – Accepted: 23 August 2018 – Published: 20 September 2018

Abstract. Somali upwelling history has been reconstructed for the last 18.5 ka BP based on biogenic silica fluxes estimated from a sediment core retrieved from the western Arabian Sea. Surface winds along the east African coast during the southwest monsoon (SWM) cause the Somali upwelling; thus, the intensity of this upwelling has been related to the variability of the SWM. Biogenic silica flux variation suggests periodic weakening and strengthening of the Somali upwelling. Weakened upwelling during the 18.5–15 ka BP period and strengthened upwelling during the Bølling–Allerød (15–12.9 ka BP) suggest the onset of the SWM. The Younger Dryas (12.9–11.7 ka BP) is marked by reduced upwelling strength, with an intensification of the Somali upwelling observed at the beginning of the Holocene and a further decline at 8 ka BP. The increase in the upwelling strength recorded since 8 ka BP suggests SWM strengthening during the latter part of the Holocene. A comparison of upwelling variations with the SWM precipitation record demonstrates a reversal in the relationship between the strength of the Somali upwelling and SWM rainfall at the beginning of the Holocene. This observed shift has been attributed to the variation in the SWM strength due to the latitudinal shift of the intertropical convergence zone (ITCZ) associated with changes in moisture sources.

1 Introduction

A large fraction of the world's population resides in the tropics, where the climate is mainly driven by monsoon rainfall. Therefore, understanding the causes of past climatic changes plays a crucial role in deciphering past, present

and future monsoon variability. India, as a tropical country comprising a significant fraction of the world's population, has an economy that is largely dependent on rainfall from the southwest monsoon (SWM); hence, slight changes in SWM rainfall can have immense societal impacts in this region. Several attempts have been made to identify the factors responsible for SWM rainfall variations, and several global phenomena, such as ENSO (El Niño–Southern Oscillation) (Goswami et al., 1999; Annamalai and Liu, 2005), the Atlantic sea surface temperature (sea surface temperature hereafter referred to as SST; Goswami et al., 2006; Yadav, 2017), Eurasian snow cover (Hahn and Shukla, 1976; Pant and Rupa Kumar, 1997; Bamzai and Shukla, 1999), the pre-monsoon 500 hPa ridge (Mooley et al., 1986), the Indo-Pacific warm pool (Parthasarathy et al., 1988, 1991), the Pacific decadal oscillation (Krishnan and Sugi, 2003), and the Atlantic multi-decadal oscillation (Krishnamurthy and Krishnamurthy, 2016) have been correlated with variations in SWM rainfall. In addition to these factors that influence the SWM, the Indian Ocean warm pool (IOWP) has been identified as the prominent source of moisture for SWM rainfall (Ninomiya and Kobayashi, 1999; Gimeno et al., 2010). During its maxima in the pre-monsoon period (April) the IOWP extends throughout the northern Indian Ocean, before reducing by almost half during the SWM (Izumo et al., 2008). The extent of the IOWP is primarily controlled by the Somali upwelling and to a lesser extent by the latent heat flux increase in the Arabian Sea during the SWM season (Izumo et al., 2008). Both the Somali upwelling and SWM rainfall are triggered by the SWM winds during boreal summer.

The upwelling of deep water during the SWM brings nutrients to the photic zone, thereby enhancing surface productiv-

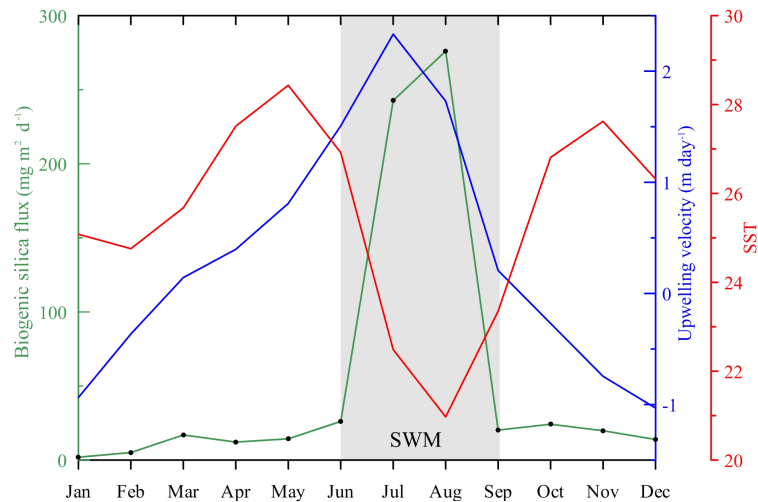


Figure 1. Modern oceanography of the western Arabian Sea. Synchronous changes in the upwelling intensity and biogenic silica flux clearly indicate that the siliceous productivity in the western Arabian Sea is controlled by SWM upwelling. Upwelling strength data are used from Yi et al. (2018) and biogenic silica flux data are used from Haake et al. (1993).

ity in the western Arabian Sea. Palaeoproductivity variations in the coastal regions off Somalia and Oman have been extensively studied in order to understand past changes in SWM-related upwelling (Sirocko et al., 1993; Naidu and Malmgren, 1996; Gupta et al., 2003; Tiwari et al., 2010). Most of these previous studies have been based on foraminifera shell abundance or chemistry. Foraminifera production persists throughout the year in the study region with maximum production during monsoon seasons. The fact that Siliceous productivity is restricted to the SWM season, means that it can serve as a better proxy than foraminifera for upwelling in the study area. Thus, variations in siliceous productivity in the western Arabian Sea have direct implications regarding the historical upwelling strength, and can be studied using the biogenic silica flux in marine sediments.

The present study aims to understand past variations in siliceous productivity in the Somali upwelling region, as well as palaeo-upwelling strength and its relationship with SWM rainfall, using a sediment core retrieved from the western Arabian Sea (Fig. 2). The surface waters of the world ocean are mostly deficient in bioavailable silica (Hurd, 1973), which is a major nutrient for siliceous productivity. Apart from the Southern Ocean, high siliceous productivity can be observed in the major upwelling regions, where upwelled nutrient-rich water causes high primary production (Koning et al., 2001). The ocean is undersaturated with respect to silica; thus, biogenic silica flux in sediments is a function of its export flux, which is controlled by its production at the surface and its dissolution in the water column as well as at the sediment–water interface (Hurd, 1973; Broecker and Peng, 1982). The use of biogenic silica as a proxy for the study of palaeo-upwelling requires an understanding of its production and burial efficiency. Sediment trap studies from

the western Arabian Sea have indicated that the biogenic silica flux mimics the SWM upwelling (Fig. 1; Haake et al., 1993). Studies of sediment trap data and surface sediments (Koning et al., 1997, 2001) from the Somali Basin provide better estimates of the burial efficiency of biogenic silica, i.e. the ratio between diatom abundance at the surface to its concentration in the sediment of the western Arabian Sea. Only 6.8%–8.7% of diatom (biogenic silica) productivity is preserved in the sediments of the Somali Basin, while the rest is remineralised in the water column and at the sediment–water interface (Koning et al., 2001). One of the major findings by Koning et al. (2001) from sediment traps in the Somali Basin is the selective preservation of upwelling indicating diatoms in the sediments of this region. This preservation is linked to the silicification of diatom frustules: most diatoms produced pre- and post-upwelling are weakly silicified, enhancing their dissolution in the water column and leading to their low preservation in the sediments. Better preservation of upwelling indicating diatoms can also be linked to the increased downward supply of biogenic silica due to high surface production. Nutrient availability (Si : N) and the concentration of dissolved iron can affect diatom silicification which leads to a variation in preservation (Hutchins and Bruland, 1998). In general, it is noted that a high silicate concentration along with a micronutrient depletion leads to more silicified and faster sinking diatoms (Hutchins and Bruland, 1998), which is also considered to be the most plausible scenario during the late phase of SWM upwelling. If burial efficiency (BE) is the primary controller of the biogenic silica flux variation, the observed ratio of low flux to low BE should be similar to the ratio of high flux to high BE. However, in the present record using the modern high and low BE values (Koning et al., 2001), the ratio of high flux to high BE (sediment core

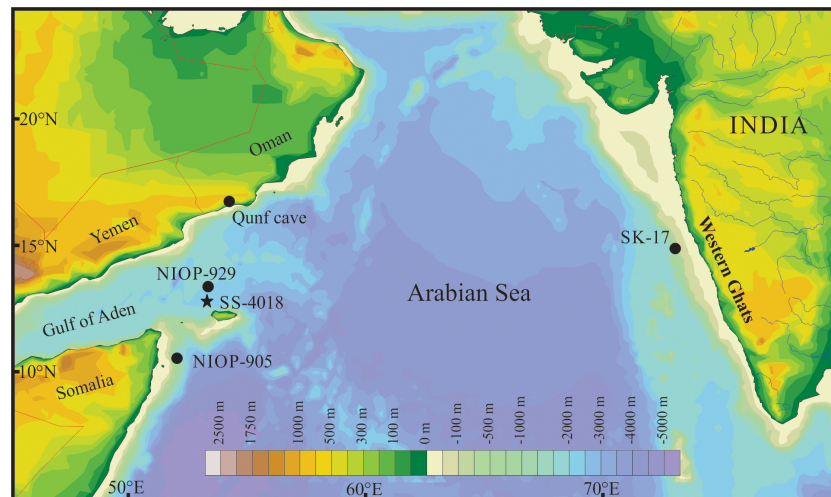


Figure 2. Location of the SS-4018 sediment core (filled star) in the Arabian Sea. The other sites discussed in the paper are also shown: NIOP-929 (Saher et al., 2007), NIOP-905 (Huguet et al., 2006), SK-17 (Anand et al., 2008) and Qunf Cave (Fleitmann et al., 2007). Map drawn with Ocean Data View (Schlitzer, 2016)

top) is almost 3 times more than the ratio of low flux to low BE (sediment core bottom). This indicates the absence of a preservation effect in the biogenic silica flux.

Apart from biogenic silica production and preservation efficiency, sediment redistribution can also influence the biogenic silica flux. However, considering the sediment core location and average sedimentation rate, it is likely that the influence of sediment focusing/winnowing on the flux record is minimal. The location of the sediment core is far from the continental slope (Fig. 2) and is not directly influenced by coastal currents or fluvial systems that would lead to the redistribution of the sediment flux. The high surface production of biogenic silica during SWM upwelling (Fig. 1; Haake et al., 1993; Koning et al., 1997), and the increased burial efficiency of upwelling indicating diatoms (biogenic silica) in the western Arabian Sea sediments (Koning et al., 2001), makes the biogenic silica flux a potential proxy for SWM-related upwelling in the study area.

1.1 Modern oceanography and productivity

The surface water circulation in the western Arabian Sea is controlled by seasonal changes in atmospheric wind patterns associated with the annual migration of the ITCZ (Wyrski, 1973). During boreal winter, the ITCZ is located south of the Equator and shifts north during boreal summer. This northward shift of the ITCZ during the southwest monsoon (SWM, June–September) season drives the Southern Hemisphere eastern trade winds across the Equator where they then turn clockwise and becomes southwest winds (Findlater, 1977; Fig. 3). These southwest winds result in the Somali current along the east African coast that moves coastal waters north. Therefore, the Somali current is generally associated with near shore upwelling and eddies such as the

southern gyre, the great whirl and the Socotra eddy (Schott et al., 1990, 2009; Beal and Chereskin, 2003). These eddies induce intense upwelling which brings low-temperature nutrient-rich subsurface water to the surface along the east coast of Africa (Young and Kindle, 1994).

Productivity in the western Arabian Sea demonstrates seasonal changes in surface ocean characteristics (Qasim, 1977; Brock et al., 1991). More than half of the annual productivity in the western Arabian Sea occurs during the SWM due to intense upwelling (Haake et al., 1993). Total flux (biogenic + dust) peaks during a similar period when productivity is at its maximum, indicating that the SWM not only results in high productivity in the western Arabian Sea but also contributes to a high dust flux (Sirocko and Lange, 1991; Haake et al., 1993). Bhushan et al. (2003) observed that the concentration of nitrate and phosphate increased at the bottom of the mixed layer at the core location, whereas a significant increase in the silicate concentration only occurred at the thermocline. During the onset of the SWM upwelling, more nitrate and phosphate than silicate reach the surface due to the upwelling of shallow waters. In the presence of high nitrate and phosphate along with micronutrients (derived by dust flux), the calcareous primary producers dominate surface productivity. Sediment trap studies in the western Arabian Sea have recorded a high biogenic carbonate flux at the onset of SWM upwelling (Haake et al., 1993). During the late phase of SWM upwelling, the surfacing of deeper waters increases the silicate concentration in surface waters. High silicate content and the depletion of micronutrients, which sustain excessive nutrient utilisation, result in siliceous productivity and a subsequent biogenic silica flux to the sediments (Fig. 1; Koning et al., 2001). Initially, this upwelled deep water surfaced at the Somali coastal upwelling zone and

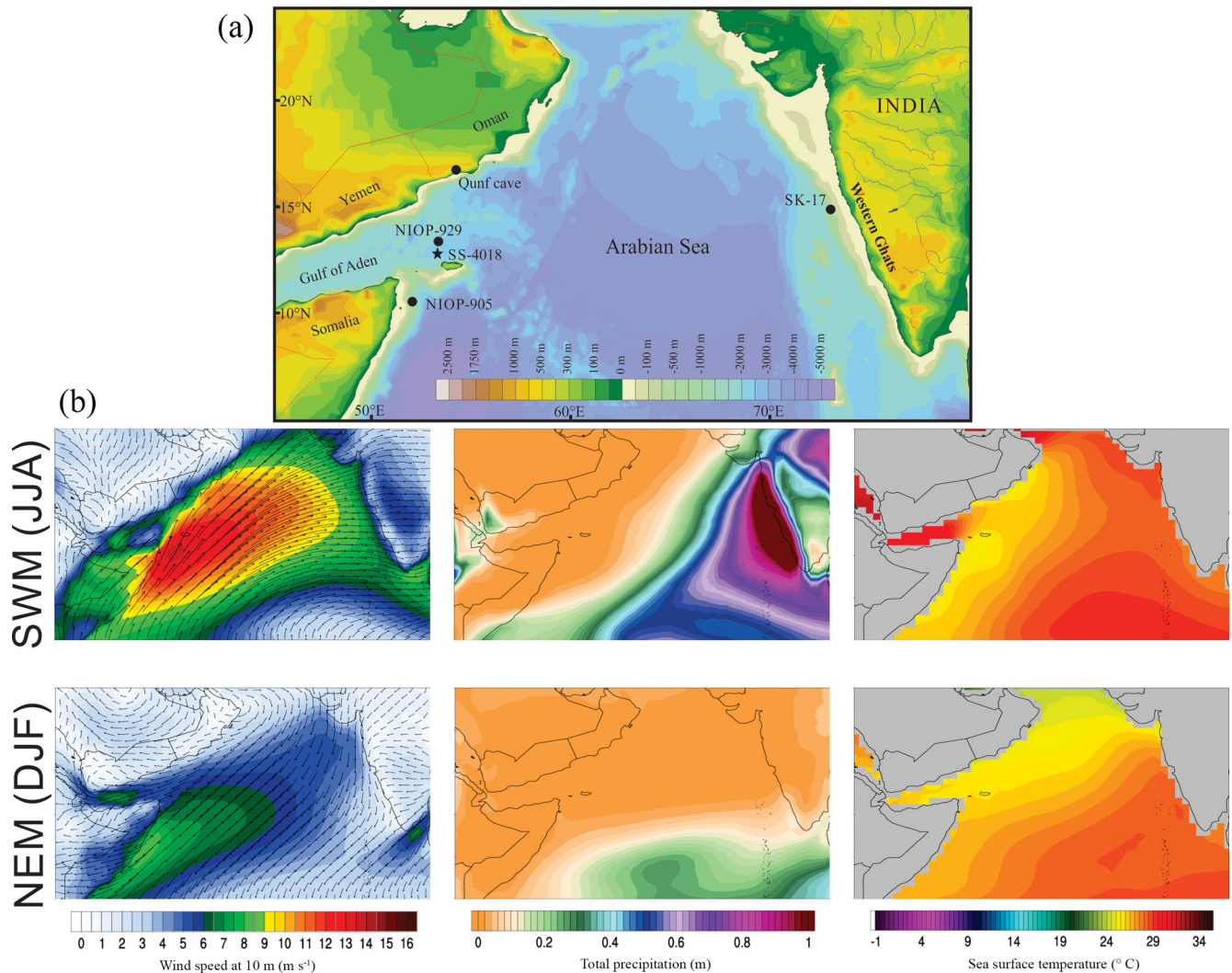


Figure 3. Location of sediment core SS-4018 in the western Arabian Sea. Sites discussed in the paper are also shown. Bottom panels show the seasonal changes in wind speed, precipitation and SST during the southwest monsoon (SWM) and the northeast monsoon (NEM). ECMWF-ERA-Interim data (Berrisford et al., 2011) were used and the images were obtained using the Climate Reanalyzer (<http://cci-reanalyzer.org>, last access: 7 May 2016), Climate Change Institute, University of Maine, USA. DJF represents December–January–February and JJA represents June–July–August.

was transported towards the mouth of the Gulf of Aden (core location) through the Socotra channel, i.e. between Socotra Island and Somalia (Young and Kindle, 1994).

2 Material and methods

Sediment core SS-4018 was collected off the Horn of Africa (north of Socotra Island), from the western Arabian Sea (13°12.80' N, 53°15.40' E; water depth 2830 m; core length 130 cm; Fig. 2) during the *FORV Sagar Sampada* cruise SS-164 in 1998. Subsampling of the core was done at 2 cm intervals. The age–depth model (Fig. 4) as well as the calcareous and organic productivity proxies of this sediment core have been presented elsewhere (Tiwari et al., 2010). Dry

bulk density (DBD) was computed using an empirical equation based on the calcium carbonate concentrations (Clemens et al., 1987). The flux rate was estimated using an average sedimentation rate computed based on the age–depth model given by Tiwari et al. (2010). The sedimentation rate at the core site, as given by Tiwari et al. (2010), is variable: the lowest rate is 3.5 and highest rate is 22.7 cm ka⁻¹. Since the age–depth model depends on the sample selection criteria and may change according to depth of age control points, in addition to the fact that the actual sedimentation at the SS-4018 sediment core site is possibly much more complex than the age–depth model presented in Tiwari et al. (2010), an average sedimentation rate was computed for the entire core.

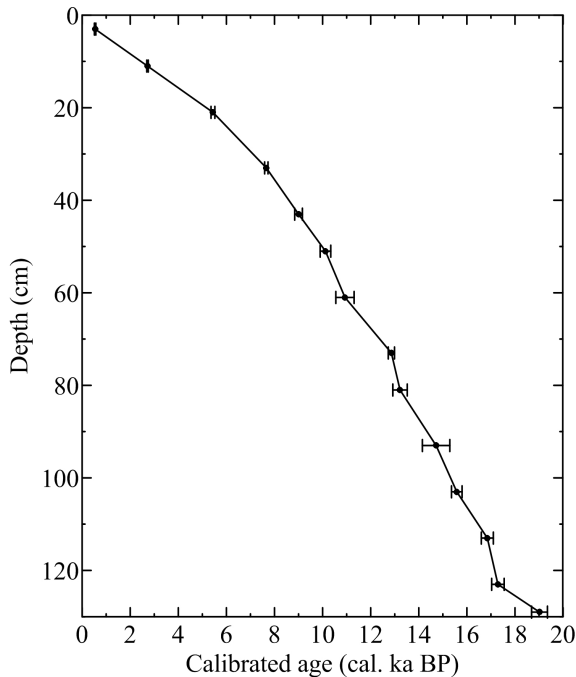


Figure 4. Age–depth model of the SS-4018 sediment core (adopted from Tiwari et al., 2010). The error bars mark 1σ uncertainty in the calibrated age.

This average age–depth model is only used to understand large-scale changes in the biogenic silica concentration.

The biogenic silica concentration was measured in each sample using the method described by Carter and Colman (1994). Dried homogenised samples weighing 50 mg were placed in centrifuge tubes. Five millilitres of 10 % H_2O_2 was added to each sample at room temperature, and the samples were stored for 2 h to remove organic matter. Five millilitres of 1 N HCl was then added to each tube. After acid treatment, samples were washed thoroughly with 20 mL of distilled water, and were then centrifuged for 15 min. Sample were kept in an oven for drying after the removal of the supernatant. Thirty millilitres of 2 M Na_2CO_3 was added to each sample, and the samples were then kept in a shaker bath at 95 °C for 5 h. After this period the samples were centrifuged, and 3 mL of hot supernatant was pipetted out of each sample and added to exactly 30 mL of distilled water in pre-cleaned sample tubes. The solution was acidified by adding 0.9 mL of concentrated HNO_3 . The sample tubes were sealed after effervescence. The silicon and aluminium concentrations were measured in these samples using inductively coupled plasma atomic emission spectroscopy (ICP-AES; Jobin-Yvon, Model 38S). The silicon concentrations were then corrected for clay mineral dissolution using the formula given by Carter and Colman (1994) (Eq. 1):

$$\Delta\text{Si} = \text{Si} - (\text{Al} \cdot 1.93), \quad (1)$$

where ΔSi is the corrected silicon concentration, Si and Al are the measured concentrations of silicon and aluminium in the sample and 1.93 is the Si to Al ratio in smectite. Smectite is an abundant clay mineral in the northern Arabian Sea (Sirocko et al., 1991). Biogenic silica concentrations were calculated using the following formula (Eq. 2):

$$\text{Biogenic silica} = \Delta\text{Si} \cdot K, \quad (2)$$

where K is a constant that equals 2.4, which accounts for the $\sim 10\%$ water content in biogenic silica (Mortlock and Froelich, 1989). Overall, the error associated with the biogenic silica measurement is less than 5 % based on repeat measurements. The biogenic silica flux is calculated by multiplying the biogenic silica fraction by the sedimentation rate (SR) and the dry bulk density (DBD) (Eq. 3):

$$\text{B.Si flux} \left(\text{g m}^{-2} \text{yr}^{-1}\right) = \text{B.Si} \cdot \text{SR} \left(\text{m yr}^{-1}\right) \cdot \text{DBD} \left(\text{g m}^{-3}\right). \quad (3)$$

The uncertainties associated with the biogenic silica concentration (B.Si) are estimated from the error in the aluminium and silicon concentrations based on repeat measurements of standard material. The maximum error in the biogenic silica concentration is within 5 %. Dry bulk density (DBD) is calculated from the CaCO_3 concentration using an empirical equation suggested by Clemens et al. (1987). The standard uncertainty in the DBD calculation is 0.091 g cm^{-3} . The uncertainty in the average sedimentation rate (SR) is 0.12 cm ky^{-1} . The uncertainty associated with the biogenic silica flux (B.Si flux) is propagated using the following equation:

$$\sigma_{\text{B.Si flux}} = \text{B.Si flux} \cdot \sqrt{\left[\left(\frac{\sigma_{\text{B.Si}}}{\text{B.Si}}\right)^2 + \left(\frac{\sigma_{\text{DBD}}}{\text{DBD}}\right)^2 + \left(\frac{\sigma_{\text{SR}}}{\text{SR}}\right)^2\right]}, \quad (4)$$

where the prefix “ σ ” stands for uncertainty. Uncertainty in the biogenic silica concentration is below 5 %. However, the uncertainty in the flux can be up to 15 %. This increase in uncertainty is due to the high standard error associated with empirical derivation of the dry bulk density.

3 Result and discussion

3.1 Biogenic silica flux vs. SST

In a similar fashion to the biogenic silica flux, the palaeo-SST can serve as a proxy for upwelling due to the fact that upwelling increases siliceous productivity with a reduction in SST. However, this inverse relationship between siliceous productivity and SST is only valid during the SWM season, and not on an annual scale. All SST proxies tend to record the annual mean signal with a varying fraction of the seasonal signal. Glacial boundary conditions have a strong influence on the annual mean SST in the Arabian Sea irrespective of monsoon upwelling (Broccoli, 2000; Dahl and Oppo, 2006). However, the biogenic silica flux is controlled by the SWM

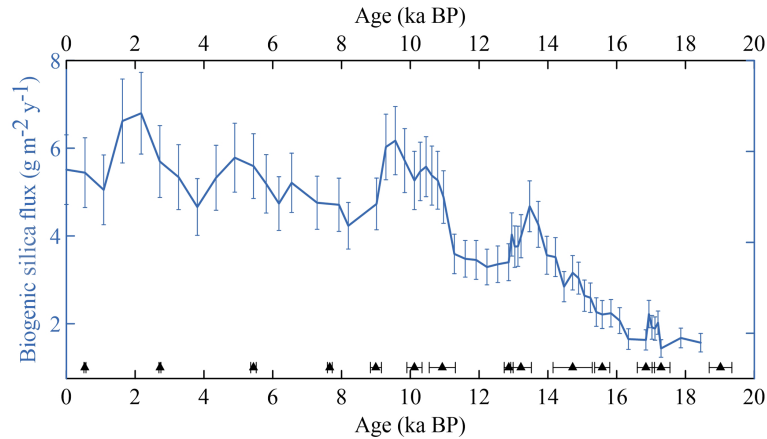


Figure 5. Temporal variation of the biogenic silica flux with 2σ uncertainty in the SS-4018 sediment core. Filled triangles at the bottom of the plot marks the age-control points with 1σ uncertainty.

Table 1. Biogenic silica concentration and flux data.

Age (ky)	B. Si (%)	σ B.Si	B.Si flux ($\text{g m}^{-2} \text{yr}^{-1}$)	σ B.Si flux	Age (ky)	B.Si (%)	σ B.Si	B.Si flux ($\text{g m}^{-2} \text{yr}^{-1}$)	σ B.Si flux
0.00	12.58	0.22	5.51	0.79	12.23	6.41	0.11	3.29	0.41
0.54	12.58	0.25	5.44	0.80	12.54	6.49	0.16	3.36	0.42
1.09	12.58	0.28	5.05	0.80	12.86	6.49	0.20	3.40	0.42
1.63	15.20	0.20	6.62	0.96	12.95	7.76	0.13	4.03	0.49
2.17	14.81	0.14	6.80	0.93	13.04	7.37	0.18	3.76	0.47
2.72	13.06	0.05	5.70	0.82	13.13	7.24	0.09	3.77	0.46
3.26	11.70	0.21	5.34	0.74	13.22	7.74	0.13	3.99	0.49
3.81	10.23	0.17	4.66	0.65	13.47	9.06	0.21	4.68	0.58
4.35	11.79	0.10	5.33	0.74	13.72	8.23	0.16	4.27	0.52
4.90	12.49	0.13	5.78	0.79	13.97	6.83	0.11	3.56	0.43
5.44	11.64	0.22	5.59	0.74	14.22	6.83	0.22	3.52	0.44
5.81	10.52	0.17	5.19	0.67	14.47	5.41	0.10	2.84	0.34
6.18	9.74	0.04	4.74	0.61	14.72	6.11	0.16	3.16	0.39
6.55	10.52	0.29	5.21	0.68	14.89	5.74	0.09	3.04	0.36
7.29	9.59	0.12	4.76	0.61	15.06	5.49	0.19	2.64	0.36
7.93	9.59	0.15	4.71	0.61	15.24	5.24	0.14	2.59	0.34
8.20	8.31	0.19	4.23	0.53	15.41	5.07	0.15	2.27	0.32
9.02	9.35	0.10	4.73	0.59	15.58	5.08	0.04	2.21	0.32
9.29	11.88	0.09	6.03	0.75	15.83	4.94	0.08	2.24	0.31
9.56	12.28	0.19	6.17	0.78	16.09	4.53	0.17	2.07	0.29
9.84	11.57	0.14	5.72	0.73	16.34	3.66	0.11	1.65	0.23
10.12	10.43	0.21	5.26	0.66	16.85	3.54	0.13	1.63	0.23
10.29	10.57	0.10	5.47	0.67	16.94	4.75	0.20	2.22	0.31
10.46	10.82	0.14	5.58	0.68	17.03	4.17	0.15	1.92	0.27
10.63	10.59	0.20	5.38	0.67	17.11	4.04	0.17	1.89	0.27
10.80	10.45	0.11	5.27	0.66	17.20	4.17	0.08	2.02	0.26
10.97	9.47	0.12	4.89	0.60	17.29	3.05	0.12	1.44	0.20
11.28	7.04	0.17	3.59	0.45	17.87	3.52	0.09	1.68	0.22
11.60	6.59	0.09	3.48	0.42	18.44	3.25	0.11	1.57	0.21
11.91	6.92	0.17	3.45	0.44					

upwelling after its production during the SWM season; therefore, it preserves the upwelling signal. Hence, the biogenic silica flux can be identified as a better proxy than SST regard-

ing understanding the SWM upwelling in the study area. The variations in biogenic silica fluxes during the last 18.5 ka are shown in Fig. 5 and the data are presented in Table 1. Com-

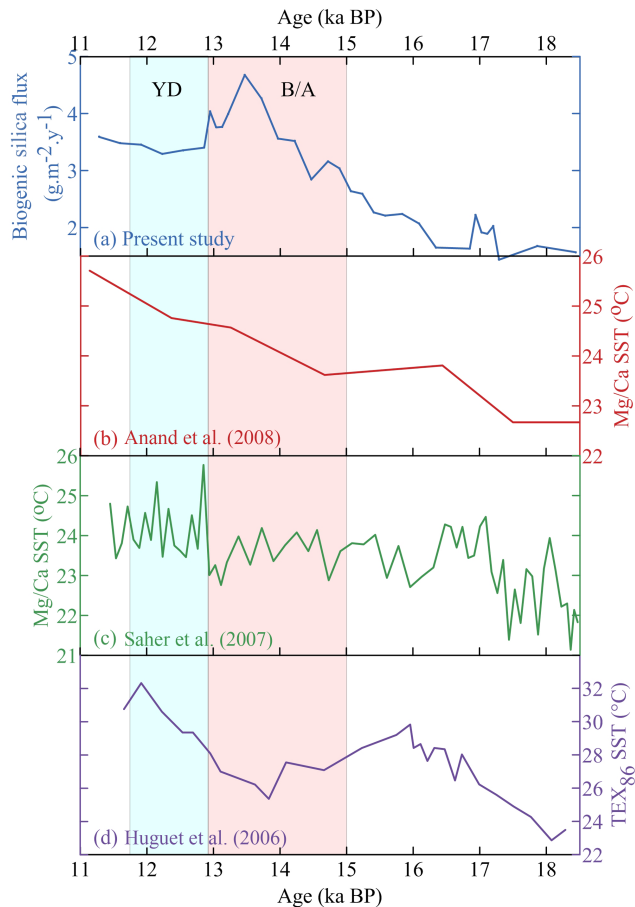


Figure 6. Comparison of the biogenic silica flux with SST records from the western Arabian Sea for the pre-Holocene period (18.5–11.7 ka BP). (a) The biogenic silica flux, (b) the Mg / Ca based SST from the NIOP-905 core (Anand et al., 2008), (c) the Mg / Ca based SST from the NIOP-929 core (Saher et al., 2007) and (d) the TEX₈₆ SST from the NIOP-905 core (Huguet et al., 2006).

Comparisons of the biogenic silica flux with other palaeo-SST records (Huguet et al., 2006; Sahar et al., 2007; Anand et al., 2008) from adjacent locations are shown in Figs. 6 and 8. No definitive relationship can be observed between the biogenic silica flux and SST records over time. The SSTs, using different proxies, show inconsistent changes during the studied time span, although the TEX₈₆ SST is always higher than the Mg / Ca SST (Figs. 6 and 8). A general observation is that both the biogenic silica flux and SST are low during the 18.5–15 ka BP period, and later show a negative correlation (Fig. 6). The negative correlation is strong between the biogenic silica flux and the TEX₈₆ SST during the 15–11.7 ka BP period (Fig. 6); however, during the last 11.7 ka the Mg / Ca based SST shows a strong negative correlation with the biogenic silica flux record, indicating a variation in the influence of the seasonal signal on different SST proxies (Fig. 8).

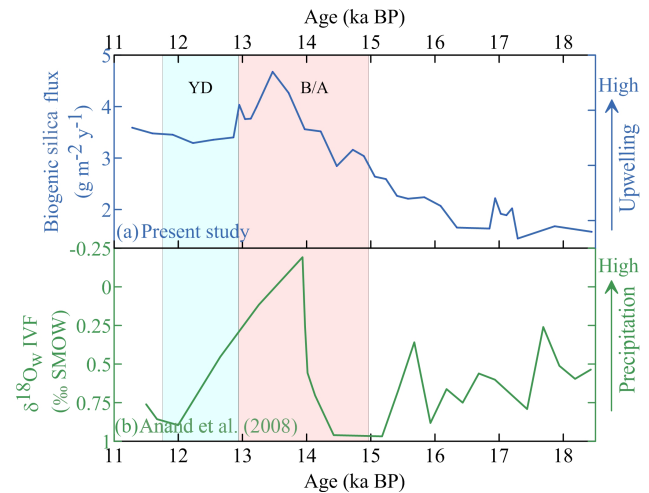


Figure 7. A comparison of the biogenic silica flux with the rainfall record from the eastern Arabian Sea for the pre-Holocene period (18.5–11.7 ka BP). (a) The biogenic silica flux (present study) and (b) $\delta^{18}\text{O}_w$ IVF (Anand et al., 2008). SMOW stands for Standard Mean Ocean Water.

3.2 Somali upwelling strength vs. southwest monsoon rainfall

Western Arabian Sea SSTs during the SWM are directly related to upwelling strength (enhanced upwelling results in lower SSTs and vice versa; Fig. 1). Previous studies have shown the northern Indian Ocean, in particular the Arabian Sea, to be an important source of moisture for SWM rainfall over India (Ninomiya and Kobayashi, 1999; Gimeno et al., 2010). Various possible relationships are observed between the SST, moisture and SWM rainfall. It is assumed that a first-order relationship would be positive, i.e. reduced SWM winds would cause reduced upwelling as well as reduced rainfall and vice versa. However, the relationship between the Arabian Sea SST and SWM rainfall is complicated due to the fact that SST modulates the moisture availability as well as the meridional temperature gradient (Levine and Turner, 2012). A modelling study by Shukla (1975) showed that the low (cold) Arabian Sea SST during the SWM tends to reduce SWM rainfall through reduced moisture transport. However, Webster et al. (1999) and Clark et al. (2000) showed that the SWM rainfall has a stronger connection with winter and spring SSTs than with summer SSTs, and suggested the delayed influence of SST on rainfall. A modelling study by Arpe et al. (1998) demonstrated that a warmer northern Indian Ocean leads to increased SWM rainfall over India through enhanced evaporation and moisture supply, while also indicating the strong influence of Pacific SST anomalies on the monsoon. It has also been suggested that the Arabian Sea SST modulates the impact of ENSO on monsoon precipitation (Arpe et al., 1998; Levine and Turner, 2012). Furthermore, an observational study by Vecchi and Harrison (2004)

detected a strong positive correlation between western Arabian SSTs and SWM rainfall over the Western Ghats mountains in India from 1982 to 2001. Overall, it has been suggested that any isolated cooling of the Arabian Sea will reduce SWM rainfall due to a reduced moisture supply, in the absence of other large-scale forcing (Levine and Turner, 2012). An observational and modelling study by Izumo et al. (2008) focused upon causes for the variations in western Arabian Sea SSTs and the influence of these variations on SWM rainfall over the Western Ghats. According to Izumo et al. (2008), increased Somali upwelling during late spring reduces the westward extension of the IOWP during summer, which decreases the moisture availability to the air mass delivering rainfall to the western part of the Indian subcontinent. However, the upwelling–rainfall connection is not fully understood and is difficult to model. Nevertheless, observations suggest a negative correlation between the Somali upwelling (western Arabian Sea SST during SWM) and SWM rainfall. Both the Somali upwelling and SWM rainfall are initiated by southwest monsoonal winds during SWM season; hence, a negative correlation indicates the negative influence of the Somali upwelling on SWM rainfall during SWM season.

Did a negative correlation exist between the Somali upwelling and SWM rainfall in the geological past? To answer this question, we need to investigate the record of palaeo-upwelling in the Somali region and palaeo-rainfall in the western part of India and adjoining areas. There is no continuous terrestrial record of palaeo-rainfall covering the last 18.5 ka from the Western Ghats, but there are several palaeo-climatic records based on marine sediment cores from the eastern Arabian Sea. The biogenic silica flux temporal variability is compared (Figs. 7 and 10) with the palaeo-rainfall record ($\delta^{18}\text{O}_w$ IVF by Anand et al., 2008) from the eastern Arabian Sea and a speleothem record from Oman (Fleitmann et al., 2003). The $\delta^{18}\text{O}_w$ IVF is the ice volume free (IVF) oxygen isotopic composition of seawater based on the $\delta^{18}\text{O}$ of *Globigerinoides ruber*. Anand et al. (2008) showed that the reconstructed $\delta^{18}\text{O}_w$ IVF during the last 19 ka from a sediment core (SK-17) in the eastern Arabian Sea was mainly regulated by the SWM rainfall in the Western Ghats. The Qunf speleothem record from Oman (Fleitmann et al., 2003) had been widely used as an indicator for SWM variation. The location of the Qunf speleothem is very close to the present study area, i.e. on the downwind side of the present research location during SWM season. If the SWM was the reason for the rainfall in southern Oman, then the western Arabian Sea must have been the source of moisture. However, there is no observational study on the relationship between upwelling strength and rainfall in Oman, although a comparison is made to give a preliminary assessment. Since records are from different regions and have irregular temporal resolution, only long-term trends have been examined.

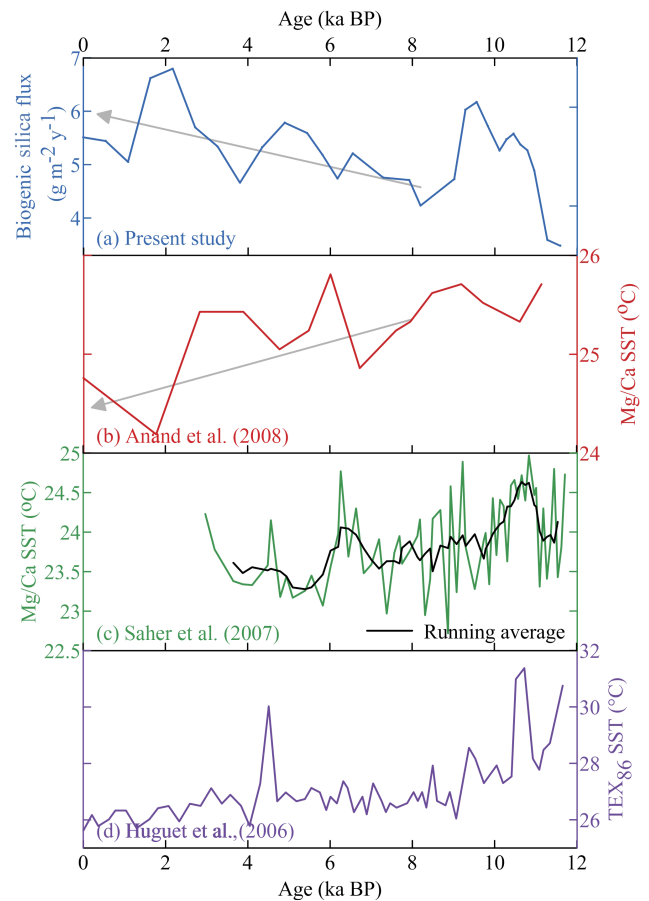


Figure 8. A comparison of the Somali upwelling with the western Arabian Sea SST records. (a) The biogenic silica flux, (b) the Mg / Ca based SST from the NIOP-905 core (Anand et al., 2008), (c) the Mg / Ca based SST from the NIOP-929 core (Saher et al., 2007) and (d) the TEX₈₆ SST from the NIOP-905 core (Huguet et al., 2006). Grey arrows indicate the trend of the proxy records during the last 8 ka.

3.2.1 Last glacial period (18.5–15 ka BP)

The biogenic silica flux record does not show any distinct variation between the previously identified Heinrich event 1 and the last glacial maximum (LGM; Clark et al., 2009). Thus, the period between 18.5 and 15 ka is considered here as the last glacial period (LGP). Both biogenic silica concentrations (3%–5%) and their fluxes ($\sim 2 \text{ g m}^{-2} \text{ yr}^{-1}$) were observed to be lowest during the LGP (Fig. 5), which is similar to previous findings regarding low productivity during glacial periods from the western Arabian Sea (Burckle, 1989; Sirocko et al., 1991, 2000; Ivanochko et al., 2005; Tiwari et al., 2010). Based on the modern pattern of biogenic silica productivity and its burial efficiency in the western Arabian Sea, the observed low fluxes of biogenic silica indicate that the Somali upwelling was very weak during the LGP. However, the lowest SST recorded in the last 18.5 ka in the Somali Basin during the LGP (Huguet et al., 2006; Saher et al.,

2007; Anand et al., 2008) is related to basin-wide cooling and is not connected with upwelling strength (Fig. 6). Dahl and Oppo (2006) observed a reduction in the Arabian Sea SST of 2–4 °C during the LGP. Thus, it is unlikely that the IOWP (SST > 28 °C) formed during this period. In absence of the IOWP, a relationship between the Somali upwelling and rainfall is not expected. The palaeo-rainfall record from the eastern Arabian Sea shows high $\delta^{18}\text{O}_w$ IVF values indicative of a reduced freshwater flux and reduced rainfall during the LGP (Fig. 7). Based on weak upwelling in the western Arabian Sea and a reduced fresh water influx to the eastern Arabian Sea, it can be concluded that the SWM was weak/absent during the LGP.

3.2.2 Deglacial period (15–11.7 ka BP)

The deglacial period (DP) is a connecting phase between two entirely different climatic periods, the LGP and the Holocene. The DP basically comprises two millennial-scale events between 15 and 12.9 ka BP and 12.9 and 11.7 ka BP. This period nearly coincides with well-known climatic events, specifically the Bølling–Allerød (B/A) and the Younger Dryas (YD). The beginning of the B/A is marked by an abrupt increase in the biogenic silica flux (Fig. 6a), which is attributed to the effect of the northern limit of the SWM, and is observed at the study site by way of a subsequent increase in the Somali upwelling strength. This is further supported by the Zr/Hf ratios in two independent sediment cores collected near the study site, which show an increasing flux of windborne dust from the Horn of Africa (an indicator of the SWM) at the onset of the B/A (Sirocko et al., 2000; Isaji et al., 2015). The reduction in the TEX₈₆ SST during the B/A in the Somali Basin (Huguet et al., 2006) also suggests increased upwelling (Fig. 5); however, the Mg/Ca SST does not show such variation (Fig. 6). The inconsistency between the two SST records (TEX₈₆ and Mg/Ca) can be related to the control on the seasonal production of the proxy material.

The depleted values in the $\delta^{18}\text{O}_w$ IVF record from the SK-17 core (Anand et al., 2008) indicate a higher influx of fresh water from the Western Ghats, caused by high SWM rainfall during the B/A (Fig. 7c). The positive correlation between the Somali upwelling (high biogenic silica flux) and SWM rainfall in the Western Ghats (high fresh water influx to the eastern Arabian Sea) during the B/A is in contrast with the present-day scenario as observed by Vecchi and Harrison (2004). Presently, the moisture source for SWM rainfall is the Arabian Sea and the central Indian Ocean warm pool (IOWP), which is affected by SWM upwelling (Izumo et al., 2008). If the central Indian Ocean was the source of moisture for SWM rainfall during the B/A, then the observed covariation would have been possible. Thus, it is proposed that the moisture source for SWM rainfall over the Western Ghats during the B/A event was different from the modern source. The other possibility of enhanced rainfall in south-

western India due to a strong NEM during the B/A is unlikely, as siliceous productivity in the western Arabian Sea related to the NEM has not been reported (Koning et al., 1997; Ramaswamy and Gaye, 2006). In contrast to the B/A, the upwelling in the western Arabian Sea was weak during the YD, as revealed by the low biogenic silica fluxes and high SSTs (Fig. 6; Huguet et al., 2006). This is in agreement with previous studies from the Arabian Sea which show decreased productivity during the YD due to a reduction in SWM (Altabet et al., 2002; Ivanochko et al., 2005). Furthermore, the high $\delta^{18}\text{O}_w$ IVF in the eastern Arabian Sea (Anand et al., 2008) caused by a low freshwater influx points to weak SWM rainfall (Fig. 7).

3.2.3 Holocene (11.7–0 ka BP)

The beginning of the Holocene is marked by an abrupt increase in the biogenic silica flux (Fig. 8a). This sudden increase in this flux between 11.7 and 9 ka BP could be due to the intensification of the SWM (extended season) resulting from a northward shift of the ITCZ, following a peak in the Northern Hemisphere solar insolation (Fleitmann et al., 2007). Somali Basin SST records (Huguet et al., 2006; Saher et al., 2007; Anand et al., 2008) also show a marginal decrease at the onset of the Holocene, but not to the levels observed during the B/A (Fig. 8). The TEX₈₆ SST shows more variation than the Mg/Ca SST at the beginning of the Holocene; however, the Mg/Ca SST is mirror image of the biogenic silica flux pattern during the Holocene, indicating the dominance of the seasonal signal in the Mg/Ca SST during this period (Fig. 8b). Based on the stable isotopic composition of organic carbon and nitrogen in the SS-4018 core, Tiwari et al. (2010) also suggested an increase in productivity during the Holocene and attributed it to the strengthening of the Somali upwelling. The synchronous changes in the biogenic silica flux with the biogenic silica/carbonate ratio (Fig. 9) indicates a change in the dominant plankton community (carbonaceous to siliceous) due to increased upwelling, as suggested by Tiwari et al. (2010). The $\delta^{18}\text{O}_w$ IVF (Anand et al., 2008) displays values similar to the YD during the early Holocene (Fig. 10c), indicating reduced rainfall (lower fresh water influx) over the Western Ghats. This negative correlation between the Somali upwelling and SWM rainfall over southwestern India during the early Holocene (11.7 to 9 ka BP), marks the establishment of the modern-day climate system. The increased Somali upwelling in the western Arabian Sea during the early Holocene (11.7 to 8 ka BP; Fig. 10a) could have reduced the IOWP extension during the SWM season, thereby resulting in lower moisture availability and subsequent reduced rainfall over the Western Ghats. The Oman speleothem record also shows decreased precipitation during the early Holocene (Fig. 10b) and supports this interpretation of low moisture availability.

At ~ 8 ka BP (Fig. 10a), compared to the early Holocene, the Somali upwelling strength decreased but persisted be-

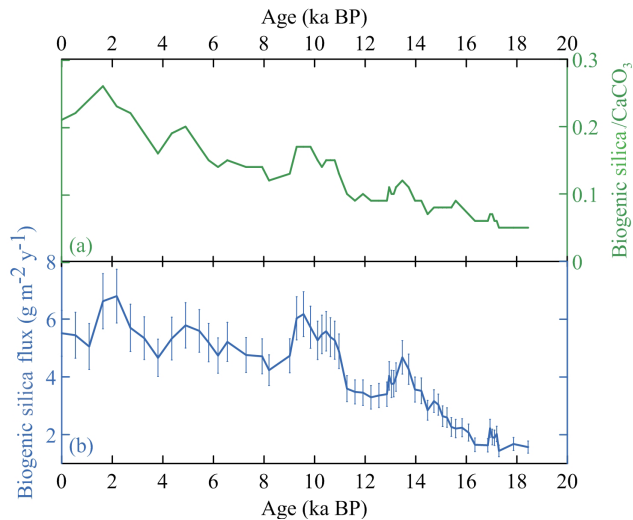


Figure 9. A comparison of the biogenic silica flux with the silica to carbonate ratio in the SS-4018 sediment core. Synchronous changes in both parameters indicate the dominance of the biogenic silica flux over the ratio.

yond YD and B/A levels, indicating the presence of the SWM with reduced wind strengths relative to the early Holocene. The SST record also shows an increased value at ~ 8 ka BP (Fig. 8b), indicating a reduction in Somali upwelling. This reduction in upwelling at 8 ka BP would have supported the westward extension of the IOWP during the SWM season, thereby increasing both moisture availability over the Arabian Sea and rainfall over the Western Ghats. The $\delta^{18}\text{O}_w$ IVF value decreased at 8 ka BP, indicating an increase in the fresh water influx from the Western Ghats (Anand et al., 2008) due to increased SWM rainfall (Fig. 10c). The Oman speleothem record also shows a decreased $\delta^{18}\text{O}$ value at 8 ka BP (Fig. 10b) suggesting increased SWM rainfall.

The Somali upwelling has undergone a gradual increase during the last 8 ka with minor positive excursion at around 5 and 2 ka BP (Fig. 10a). The increase in the SWM induced Somali upwelling during the last 8 ka contrasts with the idea that the SWM followed the Northern Hemisphere insolation during the Holocene (Gupta et al., 2003; Fleitmann et al., 2003 and references therein). However, this interpretation is in good agreement with other studies from the Arabian Sea which show that the SWM slightly increased during the Holocene (Agnihotri et al., 2003; Tiwari et al., 2010). The short-term increase in the Somali upwelling at 5 and 2 ka BP can also be observed with respect to a reduction in the Mg/Ca SST record (Fig. 8b). The Oman speleothem record shows an increase in $\delta^{18}\text{O}$ during the last 8 ka suggesting a reduction in SWM rainfall (Fig. 10b). The hiatus in the Oman speleothem record at 2 ka BP coincides with the strengthened Somali upwelling (Fig. 10a and b); this infers that the strengthened Somali upwelling at 2 ka BP might have reduced the moisture supply for the SWM rainfall over Oman

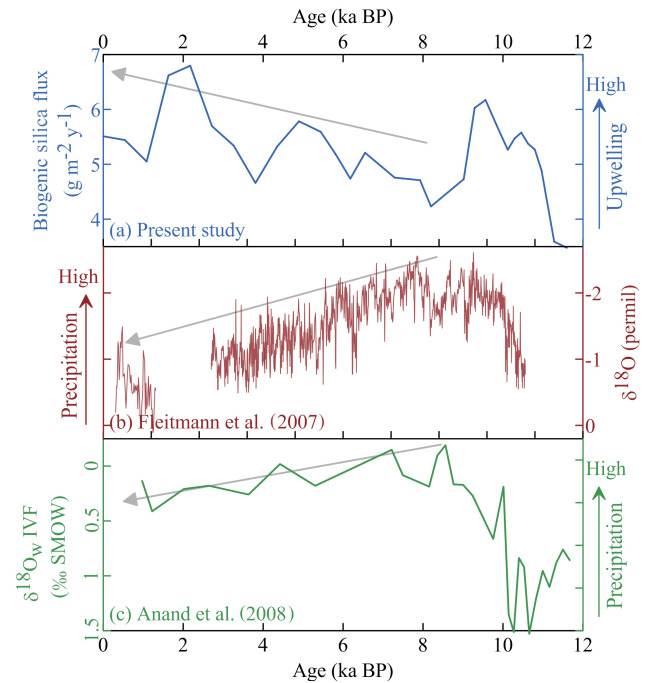


Figure 10. A comparison of the Somali upwelling with SWM rainfall records during the Holocene. (a) The biogenic silica flux (present study), (b) the Oman speleothem record and (c) $\delta^{18}\text{O}_w$ IVF data from the eastern Arabian Sea. Grey arrows indicate the trend of the proxy record during the last 8 ka.

and caused the hiatus in the speleothem record. The SK-17 record (Anand et al., 2008) shows a slight increase in the $\delta^{18}\text{O}_w$ IVF of surface waters during the last 8 ka (Fig. 10c), indicating a reduction in SWM rainfall. This opposite trend, with respect to the upwelling and rainfall record during the last 8 ka, indicates the negative impact of the Somali upwelling on SWM rainfall via the changing spatial extent of IOWP and subsequent moisture availability. However, the short-term variations in upwelling are not observed in the eastern Arabian Sea rainfall record.

It is observed that the Somali upwelling had a negative impact on SWM rainfall over southwestern India and Oman during the Holocene (except at the beginning of this period). This finding has implications in the context of the modelling study by deCastro et al. (2016), which predicts that the Somali upwelling will increase during the twenty-first century.

4 Conclusions

This study demonstrates the use of the biogenic silica flux as a proxy for temporal variations in the strength of the Somali upwelling during the last 18.5 ka. Some of the salient findings of the present study are summarised below:

1. The Somali upwelling was weak during the LGP coeval with the weak southwest monsoon (SWM).

- The post-glacial onset of the SWM was marked by an increase in the strength of the Somali upwelling at 15 ka BP, with the eastern Arabian Sea records showing increased SWM rainfall.
- The Somali upwelling was weak between 12.9 and 11.7 ka BP, indicating another weak SWM phase similar to that of the LGP. Overall, records of the Somali upwelling and SWM rainfall exhibit positive correlations between 18.5 and 11.7 ka BP.
- A shift from a positive to a negative correlation between the Somali upwelling strength and SWM rainfall occurred at 11.7 ka BP at the beginning of the Holocene, which marks the establishment of the modern-day climate system.
- Enhanced Somali upwelling during the last 11.7 ka BP, except for a decline at 8 ka BP, had a negative impact on SWM rainfall.

Data availability. Research data from this study are presented in Table 1 of this paper.

Author contributions. DB and RB developed the idea, and LSC provided overall guidance. DB performed the biogenic silica measurement from the sediment samples and wrote the paper. RB and LSC reviewed the paper.

Competing interests. The authors declare that they have no conflict of interest.

Acknowledgements. Balaji Durairaj is thankful to the Council of Scientific and Industrial Research (CSIR) of India for providing support through a CSIR-NET-Senior Research Fellowship. Ravi Bhushan thanks the director of the PRL for research grant support. We thank Alpa Sridhar for critical comments and suggestions on the paper. We thank Eduardo Zorita (editor) and three anonymous reviewers for their constructive comments which helped in improving the paper.

Edited by: Eduardo Zorita

Reviewed by: three anonymous referees

References

- Agnihotri, R., Bhattacharya, S. K., Sarin, M. M., and Somayajulu, B. L. K.: Changes in the surface productivity and subsurface denitrification during the Holocene: a multiproxy study from the eastern Arabian Sea, *The Holocene*, 13, 701–713, 2003.
- Altabet, M. A., Higginson, M. J., and Murray, D. W.: The effect of millennial-scale changes in Arabian Sea denitrification on atmospheric CO₂, *Nature*, 415, 159–162, 2002.
- Anand, P., Kroon, D., Singh, A. D., Ganeshram, R. S., Ganssen, G., and Elderfield, H.: Coupled Sea surface temperature–seawater δ¹⁸O reconstructions in the Arabian Sea at the millennial scale for the last 35 ka, *Paleoceanography*, 23, PA4207, <https://doi.org/10.1029/2007PA001564>, 2008.
- Annamalai, H. and Liu, P.: Response of the Asian summer monsoon to changes in El Niño properties, *Q. J. Roy. Meteor. Soc.*, 131, 805–831, 2005.
- Arpe, K., Dümenil, L., and Giorgetta, M. A.: Variability of the Indian monsoon in the ECHAM3 model: sensitivity to sea surface temperature, soil moisture, and the stratospheric quasi-biennial oscillation, *J. Climate*, 11, 1837–1858, 1998.
- Bamzai, A. S. and Shukla, J.: Relation between Eurasian snow cover, snow depth, and the Indian summer monsoon: An observational study, *J. Climate*, 12, 3117–3132, 1999.
- Beal, L. M. and Chereskin, T. K.: The volume transport of the Somali Current during the 1995 southwest monsoon, *Deep-Sea Res. Pt. II*, 50, 2077–2089, 2003.
- Berrisford, P., Kållberg, P., Kobayashi, S., Dee, D., Uppala, S., Simmons, A., Poli, P., and Sato, H.: Atmospheric conservation properties in ERA-Interim, *Q. J. Roy. Meteor. Soc.*, 137, 1381–1399, 2011.
- Bhushan, R., Dutta, K., Mulsow, S., Povinec, P. P., and Somayajulu, B. L. K.: Distribution of natural and man-made radionuclides during the reoccupation of GEOSECS stations 413 and 416 in the Arabian Sea: temporal changes, *Deep-Sea Res. Pt. II*, 50, 2777–2784, 2003.
- Broccoli, A. J.: Tropical cooling at the Last Glacial Maximum: An atmosphere–mixed layer ocean model simulation, *J. Climate*, 13, 951–976, 2000.
- Brock, J. C., McClain, C. R., Luther, M. E., and Hay, W. W.: The phytoplankton bloom in the northwestern Arabian Sea during the southwest monsoon of 1979, *J. Geophys. Res.-Oceans*, 96, 20623–20642, 1991.
- Broecker, W. S. and Peng, T.-H.: *Tracers in the Sea*, Lamont–Doherty Geological Observatory, Palisades, NY, USA, 1982.
- Burckle, L. H.: Distribution of diatoms in sediments of the northern Indian Ocean: Relationship to physical oceanography, *Mar. Micropaleontol.*, 15, 53–65, 1989.
- Carter, S. J. and Colman, S. M.: Biogenic silica in Lake Baikal sediments: results from 1990–1992 American cores, *J. Great Lakes Res.*, 20, 751–760, 1994.
- Clark, C. O., Cole, J. E., and Webster, P. J.: Indian Ocean SST and Indian Summer Rainfall: predictive relationships and their decadal variability, *J. Climate*, 13, 2503–2519, 2000.
- Clark, P. U., Dyke, A. S., Shakun, J. D., Carlson, A. E., Clark, J., Wohlfarth, B., Mitrovica, J. X., Hostetler, S. W., and McCabe, A. M.: The last glacial maximum. *Science*, 325, 710–714, 2009.
- Clemens, S. C., Prell, W. L., and Howard, W. R.: Retrospective dry bulk density estimates from southeast Indian Ocean sediments – comparison of water loss and chloride-ion methods, *Mar. Geol.*, 76, 57–69, 1987.
- Dahl, K. A. and Oppo, D. W.: Sea surface temperature pattern reconstructions in the Arabian Sea, *Paleoceanography*, 21, PA1014, <https://doi.org/10.1029/2005PA001162>, 2006.
- deCastro, M., Sousa, M., Santos, F., Dias, J., and Gómez-Gesteira, M.: How will Somali coastal upwelling evolve under future warming scenarios?, *Sci. Rep.-UK*, 6, 30137, <https://doi.org/10.1038/srep30137>, 2016.

- Findlater, J.: Observational aspects of low-level cross-equatorial jet stream of Western Indian Ocean, *Pure Appl. Geophys.*, 115, 1251–1262, 1977.
- Fleitmann, D., Burns, S. J., Mudelsee, M., Neff, U., Kramers, J., Mangini, A., and Matter, A.: Holocene forcing of the Indian monsoon recorded in a stalagmite from southern Oman, *Science*, 300, 1737–1739, 2003.
- Fleitmann, D., Burns, S. J., Mangini, A., Mudelsee, M., Kramers, J., Villa, I., Neff, U., Al-Subbary, A. A., Buettner, A., and Hippler, D.: Holocene ITCZ and Indian monsoon dynamics recorded in stalagmites from Oman and Yemen (Socotra), *Quaternary Sci. Rev.*, 26, 170–188, 2007.
- Gimeno, L., Drumond, A., Nieto, R., Trigo, R. M., and Stohl, A.: On the origin of continental precipitation, *Geophys. Res. Lett.*, 37, L13804, <https://doi.org/10.1029/2010GL043712>, 2010.
- Goswami, B., Krishnamurthy, V., and Annalai, H.: A broad-scale circulation index for the interannual variability of the Indian summer monsoon, *Q. J. Roy. Meteor. Soc.*, 125, 611–633, 1999.
- Goswami, B., Madhusoodanan, M., Neema, C., and Sengupta, D.: A physical mechanism for North Atlantic SST influence on the Indian summer monsoon, *Geophys. Res. Lett.*, 33, L02706, <https://doi.org/10.1029/2005GL024803>, 2006.
- Gupta, A. K., Anderson, D. M., and Overpeck, J. T.: Abrupt changes in the Asian southwest monsoon during the Holocene and their links to the North Atlantic Ocean, *Nature*, 421, 354–357, 2003.
- Haake, B., Ittekkot, V., Rixen, T., Ramaswamy, V., Nair, R., and Curry, W.: Seasonality and interannual variability of particle fluxes to the deep Arabian Sea, *Deep-Sea Res. Pt. I*, 40, 1323–1344, 1993.
- Hahn, D. G. and Shukla, J.: An apparent relationship between Eurasian snow cover and Indian monsoon rainfall, *J. Atmos. Sci.*, 33, 2461–2462, 1976.
- Hutchins, D. A. and Bruland, K. W.: Iron-limited diatom growth and Si:N uptake ratios in a coastal upwelling regime, *Nature*, 393, 561–564, 1998.
- Huguet, C., Kim, J. H., Sinningh-Damsté, J. S., and Schouten, S.: Reconstruction of sea surface temperature variations in the Arabian Sea over the last 23 kyr using organic proxies (TEX₈₆ and U₃₇K'), *Paleoceanography*, 21, PA3003, <https://doi.org/10.1029/2005PA001215>, 2006.
- Hurd, D. C.: Interactions of biogenic opal, sediment and seawater in the Central Equatorial Pacific, *Geochim. Cosmochim. Ac.*, 37, 2257IN12267-22662282, 1973.
- Isaji, Y., Kawahata, H., Ohkouchi, N., Ogawa, N. O., Murayama, M., Inoue, K., and Tamaki, K.: Varying responses to Indian monsoons during the past 220 kyr recorded in deep-sea sediments in inner and outer regions of the Gulf of Aden, *J. Geophys. Res.-Oceans*, 120, 7253–7270, 2015.
- Ivanochko, T. S., Ganeshram, R. S., Brummer, G.-J. A., Ganssen, G., Jung, S. J., Moreton, S. G., and Kroon, D.: Variations in tropical convection as an amplifier of global climate change at the millennial scale, *Earth Planet. Sc. Lett.*, 235, 302–314, 2005.
- Izumo, T., Montégut, C. B., Luo, J.-J., Behera, S. K., Masson, S., and Yamagata, T.: The role of the western Arabian Sea upwelling in Indian monsoon rainfall variability, *J. Climate*, 21, 5603–5623, 2008.
- Koning, E., Brummer, G.-J., Van Raaphorst, W., Van Bennekom, J., Helder, W., and Van Iperen, J.: Settling, dissolution and burial of biogenic silica in the sediments off Somalia (northwestern Indian Ocean), *Deep-Sea Res. Pt. II*, 44, 1341–1360, 1997.
- Koning, E., Van Iperen, J., Van Raaphorst, W., Helder, W., Brummer, G.-J., and Van Weering, T.: Selective preservation of upwelling-indicating diatoms in sediments off Somalia, NW Indian Ocean, *Deep-Sea Res. Pt. I*, 48, 2473–2495, 2001.
- Krishnamurthy, L. and Krishnamurthy, V.: Teleconnections of Indian monsoon rainfall with AMO and Atlantic tripole, *Clim. Dynam.*, 46, 2269–2285, 2016.
- Krishnan, R. and Sugi, M.: Pacific decadal oscillation and variability of the Indian summer monsoon rainfall, *Clim. Dynam.*, 21, 233–242, 2003.
- Levine, R. C. and Turner, A. G.: Dependence of Indian monsoon rainfall on moisture fluxes across the Arabian Sea and the impact of coupled model sea surface temperature biases, *Clim. Dynam.*, 38, 2167–2190, 2012.
- Mooley, D., Parthasarathy, B., and Pant, G.: Relationship between Indian Summer Monsoon Rainfall and Location of the Ridge at the 500-mb Level along 75° E, *J. Clim. Appl. Meteorol.*, 25, 633–640, 1986.
- Mortlock, R. A. and Froelich, P. N.: A simple method for the rapid determination of biogenic opal in pelagic marine sediments, *Deep-Sea Res.*, 36, 1415–1426, 1989.
- Naidu, P. D. and Malmgren, B. A.: A high-resolution record of late Quaternary upwelling along the Oman Margin, Arabian Sea based on planktonic foraminifera, *Paleoceanography*, 11, 129–140, 1996.
- Ninomiya, K. and Kobayashi, C.: Precipitation and Moisture Balance of the Asian Summer Monsoon in 1991, *J. Meteorol. Soc. Jpn.*, 77, 77–99, 1999.
- Pant, G. B. and Kumar, K. R.: *Climates of south Asia*, John Wiley & Sons, Hoboken, NJ, USA, 320 pp., ISBN: 978-0-471-94948-0, 1997, 1997.
- Parthasarathy, B., Diaz, H., and Eischeid, J.: Prediction of all-India summer monsoon rainfall with regional and large-scale parameters, *J. Geophys. Res.-Atmos.*, 93, 5341–5350, 1988.
- Parthasarathy, B., Kumar, K. R., and Munot, A.: Evidence of secular variations in Indian monsoon rainfall–circulation relationships, *J. Climate*, 4, 927–938, 1991.
- Qasim, S.: Biological productivity of the Indian Ocean, *Indian J. Mar. Sci.*, 6, 16, 122–137, 1977.
- Ramaswamy, V. and Gaye, B.: Regional variations in the fluxes of foraminifera carbonate, coccolithophorid carbonate and biogenic opal in the northern Indian Ocean, *Deep-Sea Res. Pt. I*, 53, 271–293, 2006.
- Saher, M., Jung, S., Elderfield, H., Greaves, M., and Kroon, D.: Sea surface temperatures of the western Arabian Sea during the last deglaciation, *Paleoceanography*, 22, PA2208, <https://doi.org/10.1029/2006PA001292>, 2007.
- Schlitzer, R.: Ocean Data View, available at: <https://odv.awi.de/> (last access: 11 September 2018), 2016.
- Schott, F., Swallow, J. C., and Fioux, M.: The Somali Current at the equator: annual cycle of currents and transports in the upper 1000 m and connection to neighbouring latitudes, *Deep-Sea Res. Pt. A*, 37, 1825–1848, 1990.
- Schott, F. A., Xie, S. P., and McCreary, J. P.: Indian Ocean circulation and climate variability, *Rev. Geophys.*, 47, RG1002, <https://doi.org/10.1029/2007RG000245>, 2009.

- Schouten, S., Hopmans, E. C., Schefuss, E., and Sinningh-Damsté, J. S.: Distributional variations in marine crenarchaeotal membrane lipids: A new tool for reconstructing ancient sea water temperatures?, *Earth Planet. Sc. Lett.*, 204, 265–274, 2002.
- Shukla, J.: Effect of Arabian Sea-surface temperature anomaly on Indian summer monsoon: a numerical experiment with the GFDL model, *J. Atmos. Sci.*, 32, 503–511, 1975.
- Sirocko, F. and Lange, H.: Clay-mineral accumulation rates in the Arabian Sea during the late Quaternary, *Mar. Geol.*, 97, 105–119, 1991.
- Sirocko, F., Sarnthein, M., Lange, H., and Erlenkeuser, H.: Atmospheric summer circulation and coastal upwelling in the Arabian Sea during the Holocene and the last glaciation, *Quaternary Res.*, 36, 72–93, 1991.
- Sirocko, F., Sarnthein, M., Erlenkeuser, H., Lange, H., Arnold, M., and Duplessy, J.: Century-scale events in monsoonal climate over the past 24 000 years, *Nature*, 364, 322–324, 1993.
- Sirocko, F., Garbe-Schönberg, D., and Devey, C.: Processes controlling trace element geochemistry of Arabian Sea sediments during the last 25 000 years, *Global Planet. Change*, 26, 217–303, 2000.
- Tiwari, M., Ramesh, R., Bhushan, R., Sheshshayee, M. S., Somayajulu, B. L., Jull, A., and Burr, G. S.: Did the Indo-Asian summer monsoon decrease during the Holocene following insolation?, *J. Quaternary Sci.*, 25, 1179–1188, 2010.
- Vecchi, G. A. and Harrison, D.: Interannual Indian rainfall variability and Indian Ocean sea surface temperature anomalies, in: *Earth Climate: The Ocean-Atmosphere Interaction*, edited by: Wang, C., Xie S. P., and Carton, J. A., American Geophysical Union, Geophysical Monograph, 147, 247–259, 2004.
- Webster, P. J., Moore, A. M., Loschnigg, J. P., and Leben, R. R.: Coupled ocean–atmosphere dynamics in the Indian Ocean during 1997–98, *Nature* 401, 356–360, 1999.
- Wyrtki, K.: Physical oceanography of the Indian Ocean, in: *The biology of the Indian Ocean*, 18–36, https://doi.org/10.1007/978-3-642-65468-8_3, 1973.
- Yadav, R. K.: On the relationship between east equatorial Atlantic SST and ISM through Eurasian wave, *Clim. Dynam.*, 48, 281–295, 2017.
- Yi, X., Hünicke, B., Tim, N., and Zorita, E.: The relationship between Arabian Sea upwelling and Indian Monsoon revisited in a high resolution ocean simulation, *Clim. Dynam.*, 50, 201–213, 2018.
- Young, D. K. and Kindle, J. C.: Physical processes affecting availability of dissolved silicate for diatom production in the Arabian Sea, *J. Geophys. Res.-Oceans*, 99, 22619–22632, 1994.